

# NERI Quarterly Progress Report

April 1 – June 30, 2005

Project 02-190 -- Development of a Supercritical Carbon Dioxide Brayton Cycle: Improving PBR Efficiency and Testing Material Compatibility

Chang Oh  
Richard Moore  
Thomas Lillo  
William Windes  
Terry Totemeier

July 2005

The INL is a U.S. Department of Energy National Laboratory operated by Battelle Energy Alliance



# **NERI Quarterly Progress Report**

**April 1 – June 30, 2005**

**Development of a Supercritical Carbon Dioxide Brayton Cycle: Improving PBR  
Efficiency and Testing Material Compatibility**

**Chang Oh  
Richard Moore  
Thomas Lillo  
William Windes  
Terry Totemeier**

**July 2005**

**Idaho National Laboratory  
Idaho Falls, Idaho 83415**

**Prepared for the  
U.S. Department of Energy  
Office of Nuclear Energy  
Under DOE Idaho Operations Office  
Contract DE-AC07-05ID14517**

## NERI QUARTERLY PROGRESS REPORT

**Project Title:** Development of a Supercritical Carbon Dioxide Brayton Cycle: Improving PBR Efficiency and Testing Material Compatibility

**Covering Period:** April 1, 2005 through June 30, 2005 (3<sup>rd</sup> quarter report, 2005)

**Date of Report:** July 27, 2005

**Recipient:** Kenny Osborne, DOE-ID

**Award Number:** M2SF 02-0190

**Project Number:** 02-190

**Principal Investigator:** Dr. Chang Oh  
208-526-7716, [Chang.Oh@inl.gov](mailto:Chang.Oh@inl.gov)

**Collaborators:** Richard Moore; 208-526-9671; [Richard.Moore@inl.gov](mailto:Richard.Moore@inl.gov)  
Thomas Lillo; 208-526-9746; [Thomas.Lillo@inl.gov](mailto:Thomas.Lillo@inl.gov)  
William Windes; 208-526-6985; [William.Windes@inl.gov](mailto:William.Windes@inl.gov)  
Terry Totemeier; 208-526-3074; [Terry.Totemeier@inl.gov](mailto:Terry.Totemeier@inl.gov)

**Project Objective:** The objective of this research is to improve a helium Brayton cycle and to develop a supercritical carbon dioxide Brayton cycle for the Pebble Bed Reactor (PBR) that can also be applied to the Fast Gas-Cooled Reactor (FGR) and the Very-High-Temperature Gas-Cooled Reactor (VHTR). The proposed supercritical carbon dioxide Brayton cycle will be used to improve the PBR, FGR, and VHTR net plant efficiency. Another objective of this research is to test materials to be used in the power conversion side at supercritical carbon dioxide conditions. Generally, the optimized Brayton cycle and balance of plant (BOP) to be developed from this study can be applied to Generation-IV reactor concepts. Particularly, we are interested in VHTR because it has a good chance of being built in the near future.

**Background:** The VHTR configuration is very important along with the choice of the working fluid. We started investigating a number of various VHTR configuration particularly in the power conversion unit. This will be our main focus for the year 3 activities. In conjunction with this main focus, our study will include the combined cycle, cycle with multiple reheat option, the recompression cycle, and others.

Highlights of the **third quarter activities of FY-05** are summarized below:

- A more detailed analysis for cycle efficiency and component sizing was investigated for a 3-shaft Brayton cycle. The same analyses are being performed on the combined and reheated cycle configurations.
- These power conversion units were coupled to a hydrogen production plant by an intermediate heat transport loop (IHTL) and heat transport loop heat exchanger (HTLHX). A detailed model of the IHTL was included in this study.
- A relative comparison of the heat exchanger and component sizes for a helium, CO<sub>2</sub> and 80%N<sub>2</sub>-20%He (by weight) working fluid was calculated.
- Parametric studies on the 3-shaft Brayton cycle were completed. The effects of working fluid, reactor outlet temperature, system pressure, mass flow and turbine cooling were studied. Parametric studies on the combined cycle and reheated cycle configurations are being performed.
- Long term corrosion testing (500 hour exposure) of coarse-grained MA 754 in supercritical CO<sub>2</sub> at 1000°C was completed.
- Preliminary analysis of corrosion behavior of the long term corrosion test completed which has suggested further analysis of corrosion product and the effect of corrosion on base metal composition.

#### **Status:**

##### **Task 1. Development of CO<sub>2</sub> Brayton Cycle**

Tasks 1-1, 1-2, 1-3, 1-4, and 1-5 were completed in the second and the third quarter of FY-03.

##### **Task 2. Improvement of HTGR Net Efficiency**

The objective of this task is to improve the overall plant cycle efficiency by increasing the efficiency of secondary side of the HTGR. To accomplish this task, we performed a number of HYSYS simulation to investigate a number of different cycle configurations: 3-shaft Brayton, combined, and reheated cycle. In this report, results from the 3-shaft Brayton cycle are included.

##### *Three-Shaft*

The three-shaft configuration, illustrated in Figure 1, consists of; (1) a primary loop (2) an intermediate heat transport loop in parallel with (3) the PCU with three turbines (high pressure turbine, low pressure turbine and power turbine), 4 compressors (low pressure compressor, medium pressure compressor 1, medium pressure compressor 2, and high pressure compressor) 1 precooler, 3 intercoolers and a recuperator. HYSYS (Figure 2) calculated a baseline efficiency of 49.92%, 46.67% and 49.55% for helium, CO<sub>2</sub> and 80%N<sub>2</sub>-20%He (by weight), respectively. The baseline conditions are outlined in Table 1.

Parameter	Nominal Value
Reactor outlet temp (°C)	900
Reactor outlet pressure (MPa)	7
Reactor inlet temp (°C)	500
Turbine inlet temp (°C)	886.3
Compressor inlet temp (°C)	30
IHX effectiveness	97%
Recuperator effectiveness	95%
HTLHX effectiveness	97%



## Component Sizes

Once the cycle efficiencies had been calculated, the relative sizes of the components were estimated. The actual size of the turbomachinery was not calculated but rather the work done by the machinery. HYSYS was used to calculate the energy output of the turbines, compressors and circulators. This gives some indication of the relative size of the components.

To determine the relative sizes of the heat exchanger the UA values (overall heat transfer coefficient time the heat transfer area) of the heat exchangers calculated by HYSYS were used. The U values were calculated, the heat transfer areas were determined and the volumes of the heat exchanger were calculated. Table 2 summarizes the results of the component sizing calculations.

The IHX, HTLHX, and recuperator were assumed to be printed circuit heat exchangers (PCHE) as designed by Heatric ([www.heatric.com](http://www.heatric.com)). PCHE are composed of channels chemically etched into plates. The plates are then stacked and diffusion bonded together and headers are attached to form the heat exchanger. For this study Alloy 800 with a thermal conductivity of 22 W/m-K (at 650 °C) was used as the construction material for the heat exchangers ([www.specialmetals.com](http://www.specialmetals.com)). The heat exchangers are assumed to be in counter flow to reduce the required surface area. The flow channels are assumed to be semicircular with a diameter of 3 mm, which is a representative value. From the stress analysis by Davis et. al. the pitch to diameter ratio was taken as 1.2 and the plate thickness to diameter ratio was taken as .57 for the IHX. For the HTLHX and the recuperator the pitch to diameter ratio assumed as 1.2 and the plate thickness to diameter ratio was assumed as 1.19 due to the higher pressure gradient in these heat exchangers. The overall heat transfer coefficient was calculated as

$$U = \left( \frac{1}{h_{hot}} + \frac{1}{h_{cold}} + \frac{t_{avg}}{k_{metal}} \right)^{-1},$$

where  $h_{hot}$  is the heat transfer coefficient for the hot channels,  $h_{cold}$  is the heat transfer coefficient for the cold channels,  $t_{avg}$  is the average thickness of the plates and  $k_{metal}$  is the thermal conductivity of the metal. The heat transfer coefficients were calculated using the Dittus-Boelter correlation with a leading coefficient of 0.021 for turbulent flow (INEEL 2003). For laminar flow, the heat transfer coefficients were calculated from the exact solution for fully developed flow with constant heat rate (Kays and Crawford 1980). The dimensions of the heat exchangers were then adjusted to give the expected pressure drop values.

Table 2. Component sizing summary.

<b>3-Shaft Configuration (900 °C)</b>			
	<b>CO2</b>	<b>He</b>	<b>N2/He Mix</b>
Total Turbine Work (MW)	483.4	533.1	532.4
Total Compressor Work (MW)	215.6	245.2	246.0
Total Circulator Work (MW)	15.5	15.8	16.1
Total Cycle Work (MW)	<b>714.5</b>	<b>794.1</b>	<b>794.5</b>
IHX Volume (m <sup>3</sup> )	202.1	213.0	183.8
HTLHX Volume (m <sup>3</sup> )	42.5	52.5	45.5
Recuperator Volume (m <sup>3</sup> )	125.1	130.0	204.6
Total Cycle Volume (m <sup>3</sup> )	<b>369.7</b>	<b>395.5</b>	<b>433.9</b>

For the baseline cases, the CO<sub>2</sub> component sizes are smaller than those for He or the N<sub>2</sub>/He mixture, giving CO<sub>2</sub> an advantage in cycle volume. The same advantage was found in the total cycle work for the CO<sub>2</sub> compared to the He and N<sub>2</sub>/He mixture.

### *Parametric Studies*

Parametric studies away from the baseline values of the systems were performed to determine the effect of varying conditions in the cycle. This gives some insight into the sensitivity of these cycles to various operating conditions. The parametric studies were carried out by isolating and varying a single working condition. Once the working condition was changed the cycle was optimized.

### *Working Fluids*

Helium, CO<sub>2</sub>, and an 80% nitrogen 20% helium (by weight) mixture were studied to determine the best working fluid in terms cycle efficiency and development cost. Helium is a well understood fluid and has been used in numerous studies pertaining to nuclear power. CO<sub>2</sub> has been slow in developing due to material concerns with the fluid. CO<sub>2</sub> does possess some advantages over helium such as a higher density allowing for smaller velocities than helium for the same pressure drop (Perry, R., et. al.). Despite the lower specific heat, the volumetric flow rates are smaller for CO<sub>2</sub> than for a helium cycle generating equivalent power. Therefore, the turbomachinery sizes are smaller for CO<sub>2</sub>. Copsey et. al. (2004) used this nitrogen-helium mixture for the working fluid in a combined cycle.

Helium was used as the working fluid in the primary side of the HTGR. It was chosen for its extensive use in studies of reactor thermal hydraulic and its low reactivity. Helium was used as the working fluid in the intermediate heat transport loop as specified by Davis et. al. (2005).

### *Reactor Outlet Temperature*

The reactor outlet temperature for the HTGR is limited by material concerns. Current designs such as the Arbeitsgemeinschaft Versuchsreaktor (AVR) have been operating at reactor outlet temperatures of 950°C. The Chinese HTR-10 was design to operate up to 950°C to investigate diverse power generation systems (e.g. gas turbine) and nuclear process heat applications. With current materials reactor outlet temperatures up to 1000°C can be realized but with a limited lifetime of 15 to 20 years (*Generation IV Roadmap*, 2001). Reactor outlet temperature was studied to determine the efficiency increase gained by using these higher temperatures. The reactor outlet temperature was varied from 900°C to 1000°C.

### *Mass Flow*

The effects of the secondary side mass flow were also studied. The sensitivity of the cycle to mass flow was studied to determine the effects of loss of coolant on the system. The mass flow rate was varied at 100, 95, and 90%.

## Pressure

The pressure in the secondary side was studied to establish the effects of a loss of pressure to the system. The pressure was varied at 5, 6, and 7 MPa.

## Turbine Cooling

In high temperature systems turbine cooling may be needed prolong the life of the turbines. This is done by splitting the outlet flow of the high temperature compressor. Most of the flow continues through the cycle while a fraction goes towards cooling the turbines. The split flow then cools the turbines and returns to the main flow inside the turbine (Saravanamuttoo, 1996).

A simplified model of turbine cooling was used to model the process. A single-stage turbine with cooling of the disc, stator blades and rotor blades was assumed. The mass flow to the stator blade and disc cooling add to the work in the turbine while the rotor cooling does not (Saravanamuttoo, 1996). It was assumed that since the cooling mass flow was small, the reduction in temperature of the working fluid due to cooling is neglected. Therefore, since the mass flow of the stator blade and disc cooling add to the work and their temperature difference is neglected they can be ignored in the calculation of the turbine work. The rotor cooling can be modeled as a loss of flow through the turbine. The model splits the outlet flow from the high pressure compressor with a small fraction going towards the turbine cooling and the rest continues through the cycle. It was assumed that 4% of the flow was need for the high temperature turbine and 2% was need for each additional turbine. This gives 8% for cooling in the three-shaft cycle.

## 3-Shaft Configuration Parametric Studies

Table 3 summarizes the results from the parametric studies on the 3-shaft Brayton cycle.

Table 3. Summary of parametric studies for 3-shaft Brayton cycle.

<b>3-Shaft Configuration</b>			
	<b>He</b>	<b>CO<sub>2</sub></b>	<b>N<sub>2</sub>/He Mix</b>
Baseline	49.92	46.67	49.55
Reactor Outlet Temperature (°C)			
950	51.83	49.42	51.59
1000	53.40	51.30	53.25
Mass Flow (%)			
95	49.41	44.64	48.94
90	48.70	42.16	48.10
Pressure (MPa)			
6	49.15	44.71	48.67
5	48.08	41.42	47.44
Turbine Cooling (%)			
8	47.64	43.70	47.51

Using higher reactor outlet temperatures increases the cycle efficiency for all working fluids, however, the component sizes will decrease as shown in Table 4. A decrease in mass flow will cause a decline in cycle efficiency. A decrease in pressure will also cause



a decline in cycle efficiency. The effect of turbine cooling on the cycle is decreased efficiency. This effects of the parametric studies are most prominent in the CO<sub>2</sub> cycle.

Table 4. Turbomachinery work loads for 950 °C and 1000 °C.

<b>3-Shaft Configuration</b>			
	<b>CO<sub>2</sub></b>	<b>He</b>	<b>N<sub>2</sub>/He Mix</b>
	<b>950 °C</b>		
Total Turbine Work (MW)	475	528.2	527.5
Total Compressor Work (MW)	190.4	229	229.1
Total Circulator Work (MW)	15.5	15.7	16.3
Total Cycle Work (MW)	<b>680.9</b>	<b>772.9</b>	<b>772.9</b>
	<b>1000 °C</b>		
Total Turbine Work (MW)	467.2	523.5	523
Total Compressor Work (MW)	171.4	214.9	214.7
Total Circulator Work (MW)	15.4	15.6	16.2
Total Cycle Work (MW)	<b>654</b>	<b>754</b>	<b>753.9</b>

#### *Plans for Next*

- We plan to continue work on parametric studies for the combined cycle including the hydrogen plant. Baseline cases will be established with helium working fluid and CO<sub>2</sub> and a N<sub>2</sub>/He mixture will be compared. The effects of reactor outlet temperature, system pressure, mass flow and turbine cooling will also be studied.
- We plan to continue work on parametric studies for the reheat configuration including the hydrogen plant. Baseline cases will be established with helium working fluid and CO<sub>2</sub> and a N<sub>2</sub>/He mixture will be compared. The effects of reactor outlet temperature, system pressure, mass flow, turbine cooling and number of reheat stages will also be studied.
- There are no concerns or issues.

#### Task 3. Materials Testing

The long term corrosion test of coarse-grained MA 754 was completed during the 3<sup>rd</sup> quarter and analysis of the sample has begun. The experiment and results are summarized below.

A coarse-grained MA 754 sample, in the form of a tube, was exposed to 99.5% pure CO<sub>2</sub> gas at 1000°C and 10 MPa for 500 hours. Samples were cut from the tube at 1 inch intervals along the tube length. The cross-sections were cut to expose the inner corroded surface. The samples were then mounted, polished, and analyzed utilizing a SEM. Higher corrosion rates were observed at the 2 to 3 inch location compared to the 0 to 1 inch cross-section sample (3" is the mid point of the tube). This was expected since the first 2 inches are housed in a water-cooled tube connector and the temperatures was much less than 1000°C compared to the section between 2 to 3 inches where a temperature of 1000°C existed, i.e. a steep temperature gradient existed

from the water-cooled connector to the mid point of the tube. The temperature gradient was not measured in this experiment but may be in the future.

The samples were observed in the SEM following metallographic preparation. Photomicrographs representative of each location are shown in Figure 3. Corrosion is more evident as one approaches the midpoint of the tube where the temperature was the greatest (1000°C). Close to the water-cooled ends, Figure 3a, the corrosion products appear to adhere to the base metal quite well while the corrosion products near the mid-point of the tube, Figure 3c, exhibit considerable porosity. The base metal may also even show the development of porosity under the corrosion layer. Further analysis of the porosity in the corrosion layer and the base metal is being performed to ensure it does not arise from sample preparation procedures.

Seven measurements of corrosion thickness on each sample were made to calculate average corrosion thickness after 500 hours of exposure. The average corrosion rate, expressed in microns per year, after 500 hours of exposure was then calculated. The corrosion rate for each section of the tube is shown in the last column of Table 5. The corrosion rate near the water cooled ends is quite low, as expected, and increased quite rapidly toward the midpoint of the tube. However, the corrosion rate at the mid point of the tube is still very low at ~200 microns/year (~0.2 mm/year).

The corrosion datum obtained after 500 hours of exposure is consistent with the data obtained in previous, shorter duration experiments. The corrosion rate datum determined after 500 hours of exposure has been added to the graph in Figure 4, in which the corrosion rate determined at different exposure times has been plotted. The new datum from the 500 hour test is shown in red. From this graph it is evident that the corrosion rate continues to decrease with time. It appears this trend will continue for even longer exposures, barring failure of the integrity of the corrosion layer, i.e. break away corrosion phenomenon.

Elemental analysis of the corrosion products was conducted on the 2-3 inch length sample. Five different spots, Figure 5, were selected and analyzed by EDS analysis to qualitatively determine the elemental species present in the corrosion product. From the analysis it was evident that chromium was being preferentially oxidized during the exposure to supercritical CO<sub>2</sub>. The outer most analysis area, spot #2 in Fig. 5, is almost exclusively chromium oxide, Figure 6. The limiting process, therefore, appears to be the diffusion of chromium through the corrosion layer. This would also explain the presence of porosity in the base metal, i.e. the chromium is being depleted in the near surface of the base metal, leaving behind porosity and the decreasing corrosion rate with increasing exposure time, i.e. it take longer for chromium atoms to diffuse through the growing corrosion layer. Further quantitative analysis of this sample will be performed next quarter to reveal the chromium depletion in the near surface region of this sample.

Table 5. Corrosion Layer Thickness in Supercritical CO<sub>2</sub>.

Sample	Corrosion Thickness, $\mu\text{m}$	
	500 Hrs (Experimental)	Year 1 (Calculated)
0 to 1 inch	0.4	7.0
1 to 2 inch	4.7	81.7

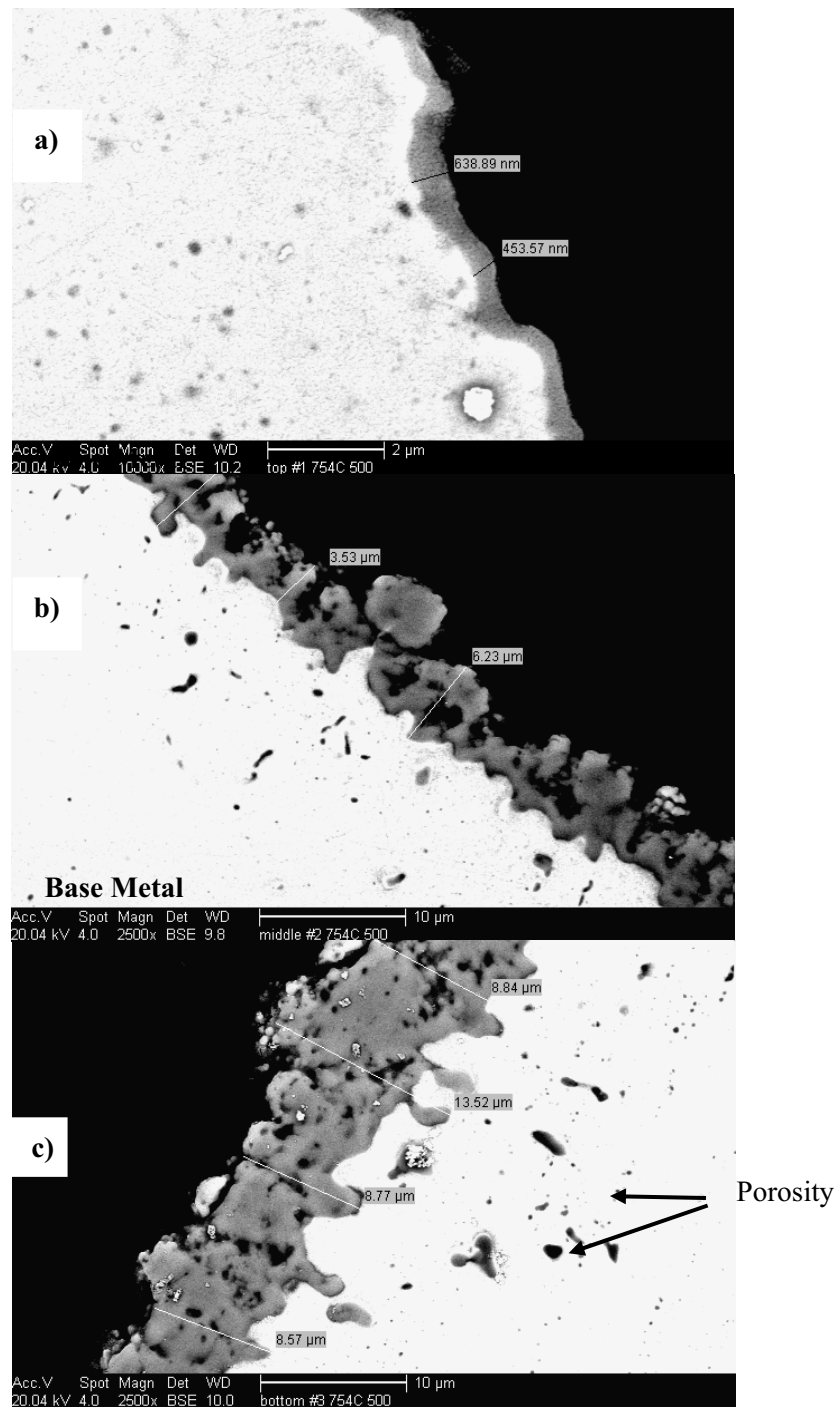


Figure. 3 SEM photographs of each section of the tube sample after 500 hours of exposure. Samples were taken from the a) 0-1", b) 1-2" and c) 2-3" sections of the tube.

2 to 3 inch	10.5	184.0
----------------	------	-------

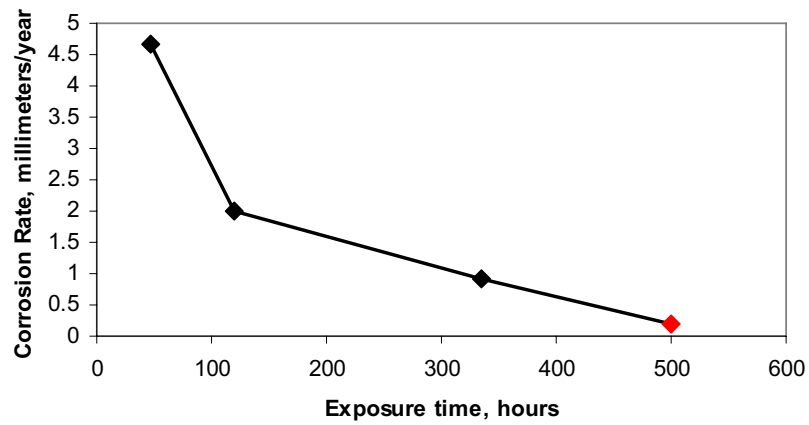


Figure 4. Corrosion rates of MA 754 in supercritical CO<sub>2</sub> at 1000°C as a function of exposure time.

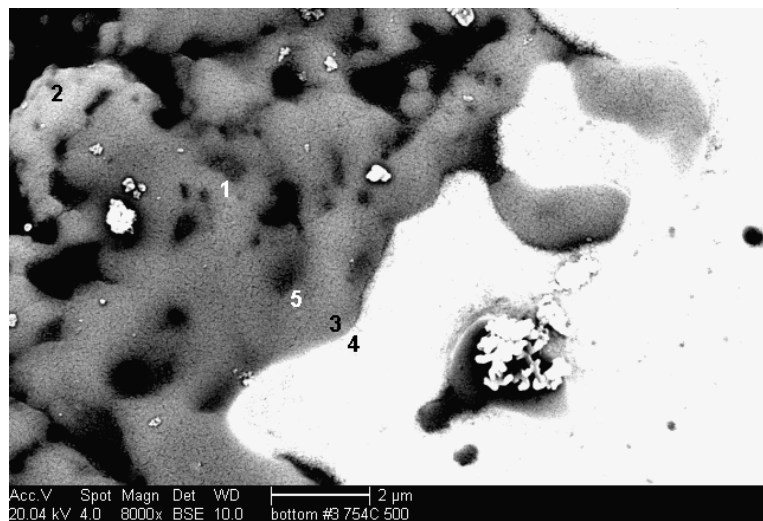


Figure 5. (BSE) Corrosion in the 2-3 inch length showing EDS analysis locations.

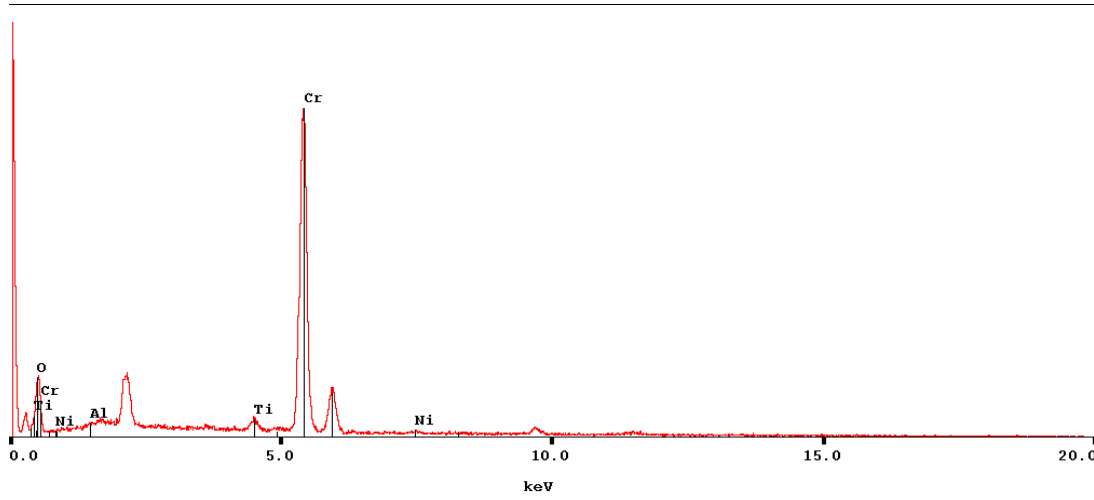


Figure 6. Elemental analysis by EDS showing the corrosion product at the outermost #2 location is almost exclusively chromium oxide.

#### *Plans for Next*

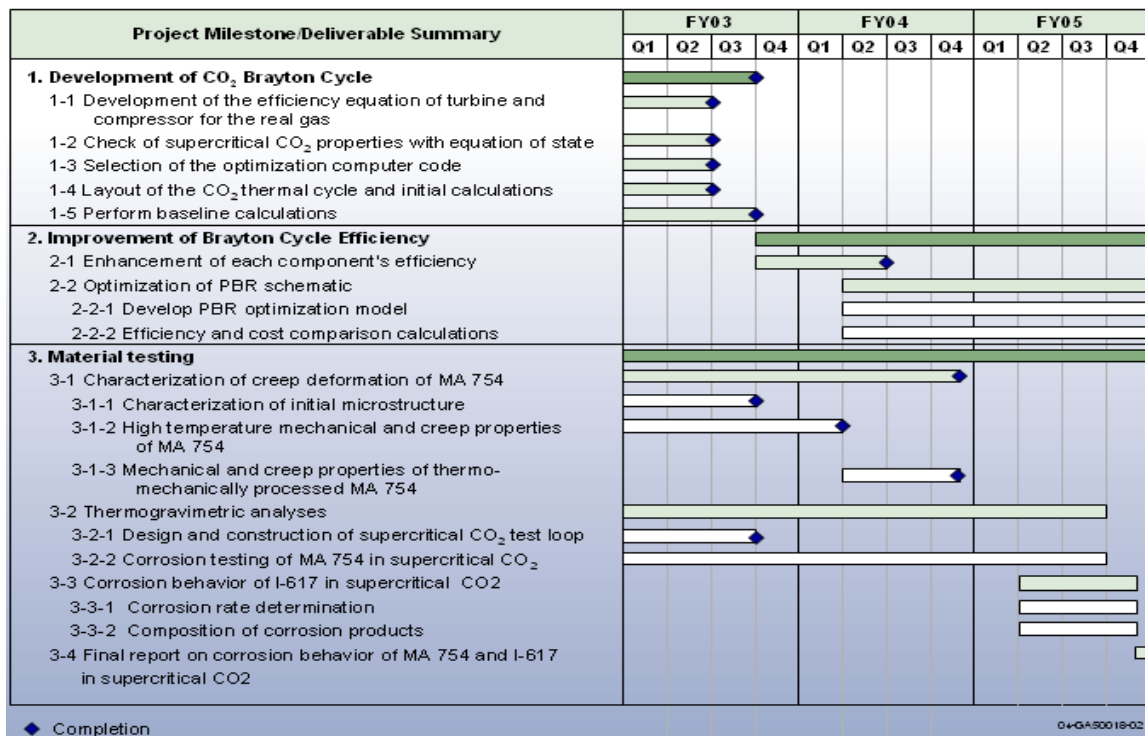
- Analyze the effect of corrosion on chromium concentration in the base metal to identify corrosion mechanism.
- Prepare manuscript on the corrosion behavior of coarse-grained MA 754
- Begin corrosion testing of fine-grained MA 754
- Begin corrosion testing of I-617
- Prepare final report on the corrosion behavior of MA 754 (coarse-grained and fine-grained) and I-617 in supercritical CO<sub>2</sub>
- No concerns

#### **Project Milestones:**

The project milestones are shown below:

<b>Milestone/Deliverable Description</b>	<b>Planned Completion</b>	<b>Actual Completion</b>
1. Development of CO <sub>2</sub> Brayton Cycle	30 June 2003	Completed
1-1 Development of the efficiency equation of turbine and compressor for the real gas	31 March 2003	Completed
1-2 Check of supercritical CO <sub>2</sub> properties with equation of state	31 March 2003	Completed
1-3 Selection of the optimization computer code	31 March 2003	Completed
1-4 Layout of CO <sub>2</sub> thermal cycle and initial calculations	31 March 2003	Completed
1-5 Perform baseline calculations	30 June 2003	Completed
2. Improvement of Brayton cycle efficiency	30 September 2005	In progress
2-1. Enhancement of each component's efficiency	31 March 2004	Completed
2-2. Optimization of PBR schematic	30 September 2005	In progress

2-2-1 Develop PBR optimization model	30 September 2005	In progress
2-2-2 Efficiency and cost comparison calculations	30 September 2005	In progress
3. Material testing	30 September 2005	In progress
3-1 Characterization of creep deformation of MA 754	30 September 2004	Completed
3-1-1 Characterization of initial microstructure	30 June 2003	Completed
3-1-2 High temperature mechanical and creep properties of MA 754	31 December 2003	Completed
3-1-3 Mechanical and creep properties fine-grained MA 754	31 August 2004	Completed
3-2 Thermogravimetric analyses	30 September 2005	In progress
3-2-1 Design and construction of supercritical CO <sub>2</sub> test loop	30 June 2003	Completed
3-2-2 Corrosion testing of MA 754 in supercritical CO <sub>2</sub>	30 September 2005	In progress
3-3 Corrosion behavior of I-617 in supercritical CO <sub>2</sub>	31 August 2005	Starts 4 <sup>th</sup> quarter of FY05
3-3-1 – Corrosion rate determination	31 August 2005	In progress
3-3-2 – Composition of Corrosion products	31 August 2005	In progress
3-4 Final report on corrosion behavior of MA 754 and I-617 in supercritical CO <sub>2</sub>	30 September 2005	Starts 4 <sup>th</sup> quarter of FY05



## Appendix:

## References

Aspen Technology, *HYSYS Process Version 2.2.2*, [www.aspentech.com](http://www.aspentech.com), 2005.

Copsey, B., M. Lecomte, G. Brinkmann, A. Capitaine, and N. Deberne, *The Framatome ANP Indirect-Cycle Very High Temperature Reactor*, Proceedings of ICAPP '04, Paper 4201, June 2004.

Davis, C., O. Chang, R. Barner, S. Sherman and D. Wilson, *Thermal-Hydraulic Analyses of Heat Transfer Fluid Requirements and Characteristics for Coupling A Hydrogen Production Plant to a High-Temperature Nuclear Reactor*, INL/EXT-05-00453, June 2005.

Dostal, V., M. J. Driscoll, and P. Hejzlar, *A Supercritical Carbon Dioxide Cycle for Next Generation Nuclear Reactors*, MIT-ANP-TR-100, March 2004.

*Generation IV Roadmap, Description and Evaluation of Candidate Gas-Cooled Reactor Systems*, TWG-2, Summary Prt XR01-03, December 2001.

Heatric, [www.heatric.com](http://www.heatric.com), 2005.

INEEL, *RELAP5-3D Code Manual Volume 4: Models and Correlations*, INEEL-98-00834, Revision 2.2, 2003.

Kayes, W. M., and M.E. Crawford, *Convective Heat and Mass Transfer*, Second Edition, McGraw-Hill Book Company, New York, 1980.

Perry, R., D. Green, and J. Maloney, *Perry's Chemical Engineer's Handbook*, Sixth Edition, McGraw-Hill, 1984.

Saravanamuttoo, H. et al., 1996, *Gas Turbine Theory*, Fifth Edition, Prentice Hall

Special Metals, [www.specialmetals.com](http://www.specialmetals.com), 2005.

### Budget Data:

Phase / Budget Period			Approved Spending Plan	Actual Spent to Date
			Total	Total
	From	To		
Year 1	9/01/02	9/30/03	\$290,520	\$286,490
Year 2	10/01/03	9/30/04	\$302,265 (\$298,353 + \$3,912 from carry-over)	\$310,204
Year 3	10/01/04	2/29/06	\$312,402	\$169,636 (3rd quarter)

